Superconducting and hybrid circuits for quantum information processing

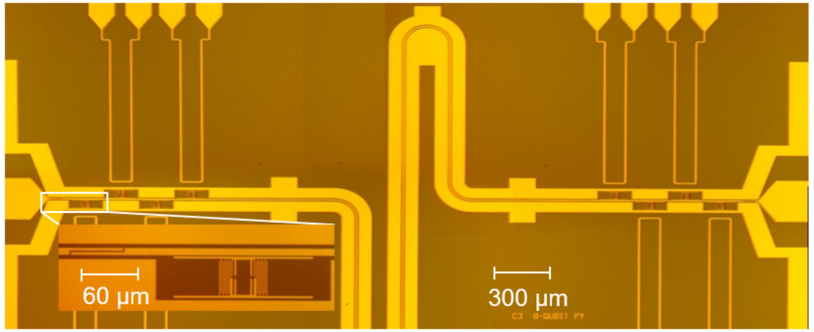

P. Yang *et al.*, arXiv:1810.00652 (2018)

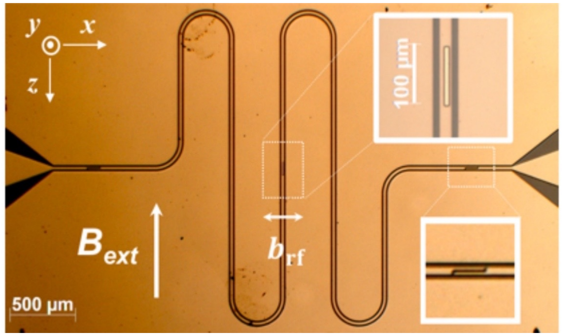

J. Hou *et al.*, PRL **123**, 107702 (2019)

Project title:

Ferromagnetic systems probed in milliKelvin temperatures using microwave spectroscopy

João Barbosa
Eng. Física

Supervisor:
Prof. Martin Weides
Prof. Fernando Nogueira

Outline

- Superconducting quantum circuits
  - Resonators and Qubits
- Hybrid interface
  - Ferromagnetic spin systems
  - Photon-magnon, magnon-qubit couplings
- Project
  - Characterization of ferromagnetic resonance at room and mK temp.

Superconducting transmission lines

- Zero DC resistivity
- Finite but very low dissipation at high frequencies below superconducting gap (Mattis-Bardeen equation)
- Common materials: Al, Nb (f_Δ ≈700 GHz, T_c ≈9K), NbTi, NbN
- CPW, stripline, microstrip designs

Superconducting resonators

- Two architectures probed:
  - lumped-element and
  - half/quarter-wavelength ($\lambda/2$, $\lambda/4$) resonators
- Lumped-element based on classical LC resonators
- $\lambda/2$ and $\lambda/4$ resonators based on microwave transmission line geometry
- High quality factors resonators ($Q \sim 10^6$)

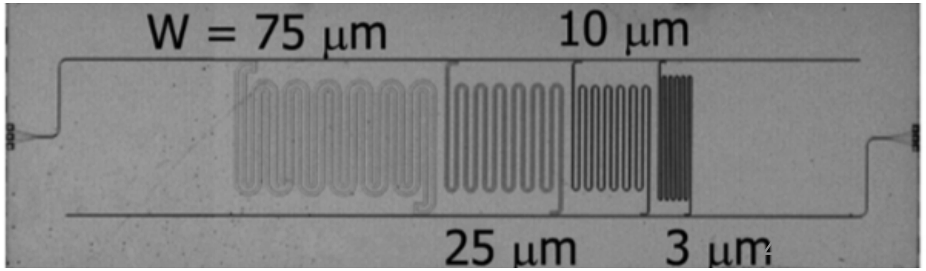

Josephson junctions

- Two superconducting layers separated by a weak link (insulator, constriction, normal metal)
- Junctions for qubits: $Al/ AlO_x /Al$
- Josephson equations characterize the behaviour of junction:

$$I = I_c \sin\varphi \qquad \text{(DC)}$$

$$\frac{\partial\varphi}{\partial t} = \frac{2e}{\hbar} V \qquad \text{(AC)}$$

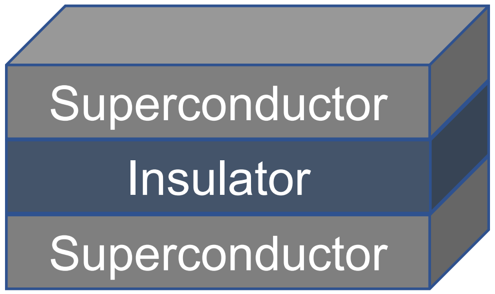

- Combining these equations:

$$V = L_J \frac{\partial I}{\partial t} \Rightarrow L_j(\varphi) = \frac{\hbar}{2e} \frac{1}{I_c \cos \varphi}$$

- JJs act as non-linear inductors with inductance dependant on critical current and phase difference
- Complex dynamics (large signals) – RCSJ model →

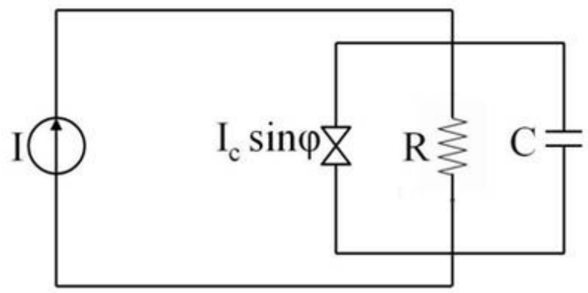

↓

Quantum computing

Create artificial anharmonic energy levels (qubits!).

SFQ Digital electronics

Generate, propagate and detect picosecond waveforms.

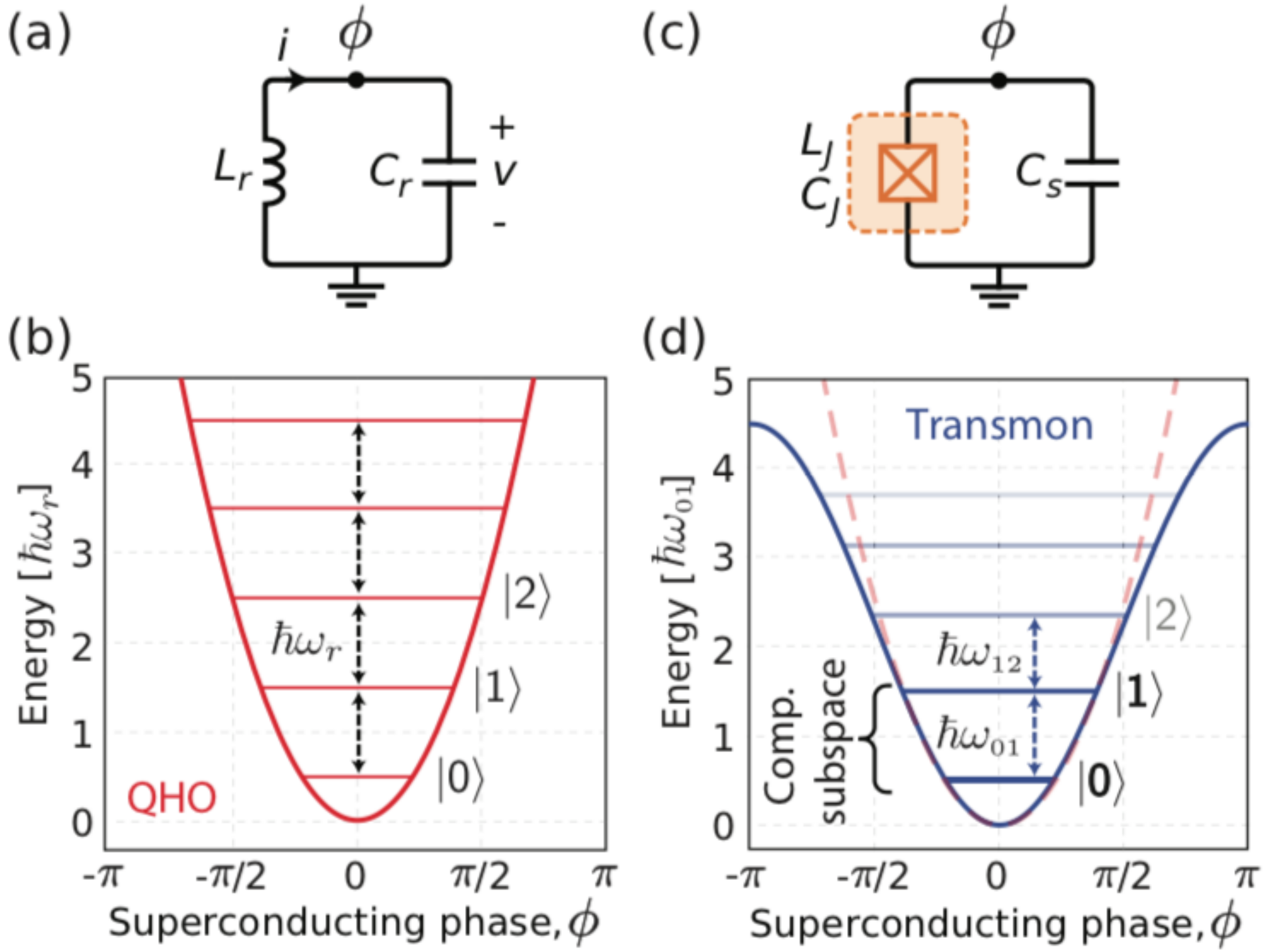

$$H = 4E_C n^2 - E_J \cos(\phi),$$

$$H = 4E_C n^2 - \underbrace{2E_J \left|\cos\left(\varphi_e\right)\right|}_{E'_J(\varphi_e)} \cos(\phi).$$

P. Krantz *et al.*, APR **6**, 021318 (2019)

SC qubit architectures

Transmon

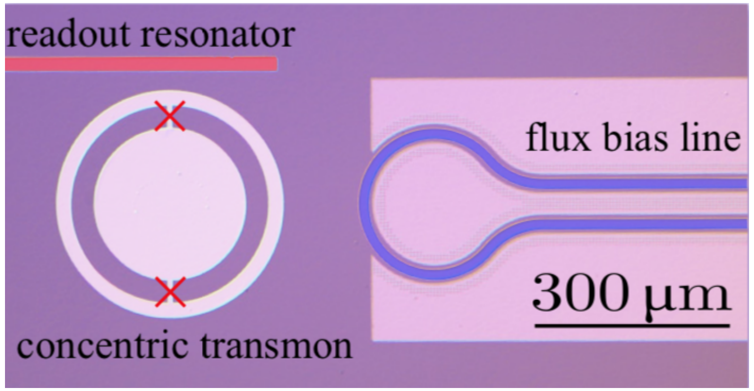

J. Braumüller *et al.*, APL **108**, 032601 (2016)

Xmon

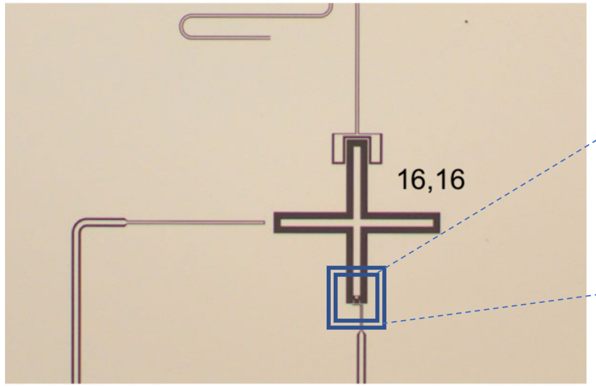

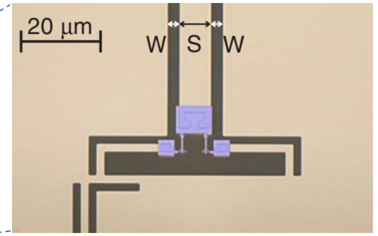

R. Barends *et al.*, PRL **111**, 080502 (2013)

- Transmon qubit architecture consists of JJ shunted by large capacitor
- Tuneable qubits achieved by using shunted JJ (DC-SQUID)
- Frequency tuned by applied external magnetic field (flux bias lines)

Qubit manipulation

Readout

- Dispersive readout of resonator coupled to qubit (non-demolition measurement)
- Resonator frequency shifts depending on the qubit state
- Drive tone (VNA)

Control

- Logical gates are realized by on or near-resonant microwave pulses with defined length and amplitude (AWG)
- Single qubit gates require qubit-qubit interaction to be turned off
- Qubit-qubit interaction mediated by resonator (“quantum bus”)

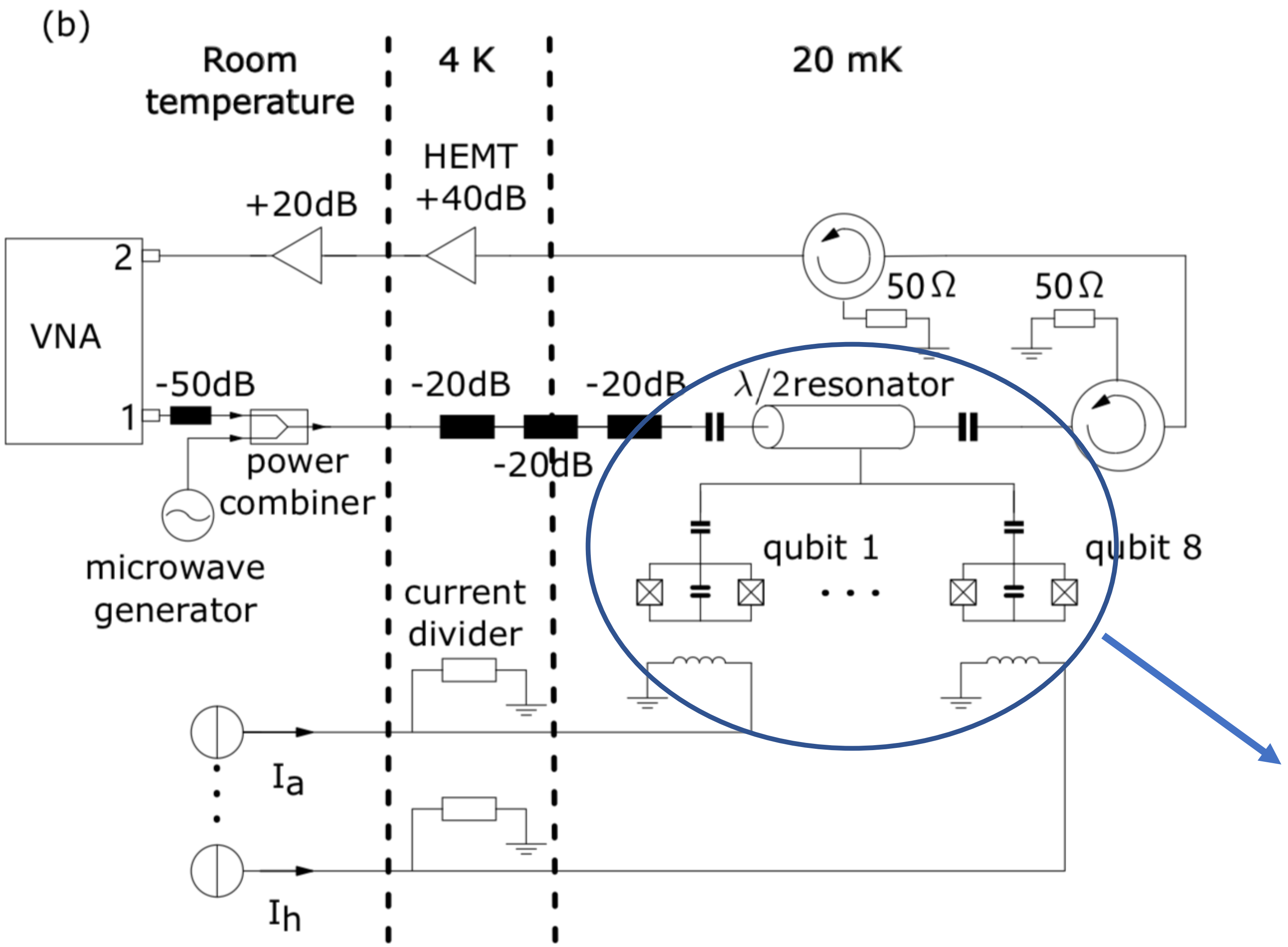

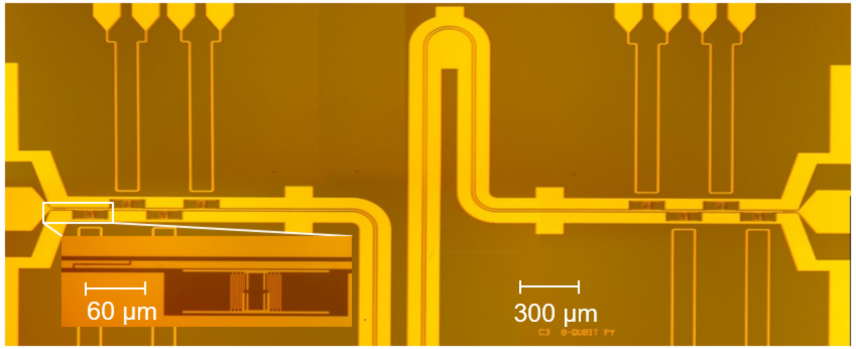

P. Yang *et al.*, arXiv:1810.00652 (2018)

Quantum computing

- QC better at solving specific problems than classical ones (quantum simulation and chemistry, adiabatic quantum optimization, Shor's algorithm…)
- Still too few qubits (and too noisy) to perform useful calculations

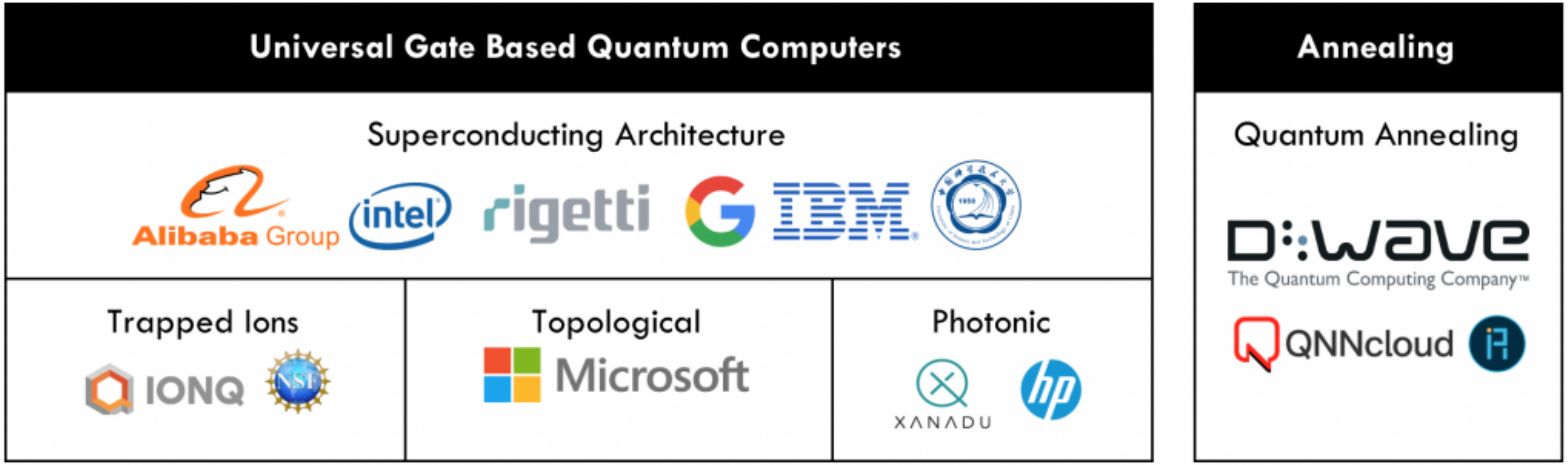

https://www.creativedestructionlab.com/2018/12/the-state-of-quantum-computing/

TABLE I. Comparison between different systems used as qubits.

	Atom, molecule, ion	Electron spin	Nuclear spin	Superconducting qubit
Size	$\sim 10^{-10}$ m	$\sim 10^{-10}$ m (impurities) $\sim 10^{-8}$ m (quantum dot)[a]	$<10^{-10}$ m[a]	$\sim 10^{-6}$ m
Energy gap	10^5–10^6 GHz, ~GHz (Rydberg atoms)	1–10 GHz	1–10 MHz	1–20 GHz
Frequency range	Optical, microwave	Microwave	Microwave	Microwave
Operating temperature	nK to μK	~100 mK (quantum dot), room temperature (NV center)	~mK	~10 mK
Single-qubit gate operation time τ_1	~μs (atom) ~50 ps (ion)	~10 ns	>10 μs	~1 ns
Two-qubit gate operation time τ_2	~μs (atom) ~100 μs (ion)	~0.2 ns	~10 ms	~10–50 ns
Coherence time T_2	ms to s	ms to s	~s	~10–100 μs
T_2/τ_1	10–10^4	10^5–10^8	10^6	10^4–10^5
Coupling type	Electric or magnetic	Magnetic or electric	Magnetic	Electric or magnetic
Coupling strength with the cavity	<kHz (B field), ~10 kHz (E field), ~10 MHz (Rydberg atoms)	>MHz (quantum dot) ~100 Hz (impurities)	~0.1 Hz	~0.1–1 GHz

- Superconducting qubits offer scalability, ease of fabrication, short quantum gate times compared to other architectures

Relatively low coherence times remain an obstacle

Xiang et al 2013 Rev. Mod. Phys., 85, 623-653.

Hybrid circuits

- Superconducting circuit + non-superconducting system strongly coupled
- Goal: take advantage of each system's strengths

Quantum memory

- Spin systems have higher coherence times.
- Transfer of quantum information through strongly coupled systems.

M. Neeley *et al.*, Nature Physics **4**, 532-526 (2008)

Optical-Microwave converters

- Possibility to create quantum networks
- Long distance transfer of quantum information from on-chip qubit to optical fibres.

R. Hisatomi *et al.*, PRB **93**, 174427 (2016)

Ferromagnetic spin systems

- Strongly interacting electrons (electrostatic, Pauli’s exclusion) with spin create domains where all spins are oriented in same direction (magnetism)

- Magnon - quantum of collective excitations of spins in magnetic materials

$$\hat{\mathcal{H}} = -g\mu_B B_z \sum_i \hat{S}_i^z - 2J \sum_{\langle i,j \rangle} \hat{\mathbf{S}}_i \cdot \hat{\mathbf{S}}_j$$

Exchange interaction!

Second quantization

$$\hat{\mathcal{H}} = \sum_{\mathbf{k}} \hbar\omega_{\mathbf{k}} \hat{c}_{\mathbf{k}}^{\dagger} \hat{c}_{\mathbf{k}}$$

Hybrid coupling

Magnons ⟷ MW photons

- Magnetostatic modes

$$\hat{\mathcal{H}}_{\mathrm{m}}/\hbar = \sum_{\mathbf{k}} \omega_{\mathrm{m}}(\mathbf{k}) \hat{c}_{\mathbf{k}}^{\dagger} \hat{c}_{\mathbf{k}}$$

- Resonating modes

$$\hat{\mathcal{H}}_{\mathrm{c}}/\hbar = \omega_{\mathrm{c}} \hat{a}^{\dagger} \hat{a}$$

$$\hat{\mathcal{H}}_{\mathrm{m-c}}/\hbar = \sum_{n} g_{\mathrm{m-c}}^{(n)} \left(\hat{a}^{\dagger} \hat{c}_n + \hat{a} \hat{c}_n^{\dagger} \right)$$

$$\hbar g_{\mathrm{m-c}} \propto \sqrt{N}$$

(Magnetic dipole interaction)

Hybrid coupling

MW photons ⟷ Superconducting qubits

- Resonating modes

$$\hat{\mathcal{H}}_\mathrm{c}/\hbar = \omega_\mathrm{c}\hat{a}^\dagger\hat{a}$$

- Qubit energy levels

$$\hat{\mathcal{H}}_\mathrm{q}/\hbar = \left(\omega_\mathrm{q} - \frac{\alpha}{2}\right)\hat{q}^\dagger\hat{q} + \frac{\alpha}{2}\left(\hat{q}^\dagger\hat{q}\right)^2$$

$$\hat{\mathcal{H}}_\mathrm{q-c}/\hbar = g_\mathrm{q-c}\left(\hat{q}^\dagger\hat{a} + \hat{q}\hat{a}^\dagger\right)$$

(Electric dipole interaction)

Hybrid coupling

Magnons

g_{m-c}

MW photons

- Magnetostatic modes

$$\hat{\mathcal{H}}_{\mathrm{m}}/\hbar = \sum_{\mathbf{k}} \omega_{\mathrm{m}}(\mathbf{k}) \hat{c}_{\mathbf{k}}^{\dagger} \hat{c}_{\mathbf{k}},$$

- Resonating modes

$$\hat{\mathcal{H}}_{\mathrm{c}}/\hbar = \omega_{\mathrm{c}} \hat{a}^{\dagger} \hat{a}$$

g_{m-q}

g_{q-c}

Superconducting qubits

- Qubit energy levels

$$\hat{\mathcal{H}}_{\mathrm{q}}/\hbar = \left(\omega_{\mathrm{q}} - \frac{\alpha}{2}\right) \hat{q}^{\dagger} \hat{q} + \frac{\alpha}{2} \left(\hat{q}^{\dagger} \hat{q}\right)^{2}$$

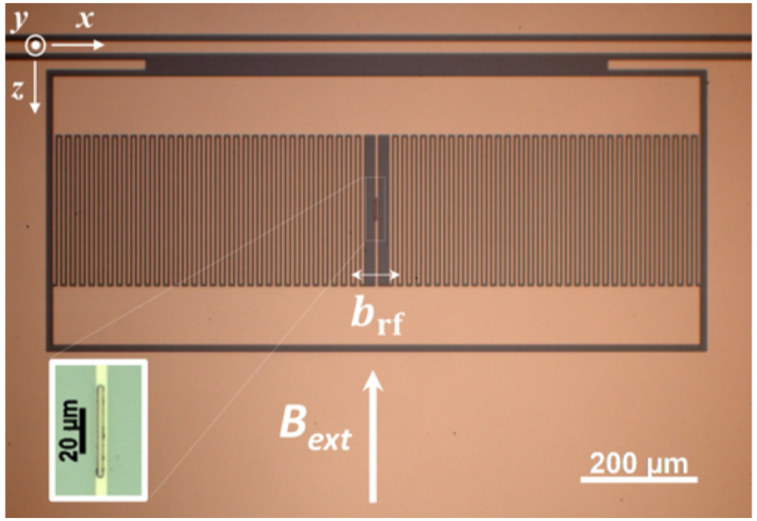

J. Hou *et al.*, PRL **123**, 107702 (2019)

- Permalloy (Ni-Fe) film
- CPW/ Lumped-element resonator

- YIG (Yttrium Iron Garnet) sphere
- Transmon qubit
- 3D microwave cavity

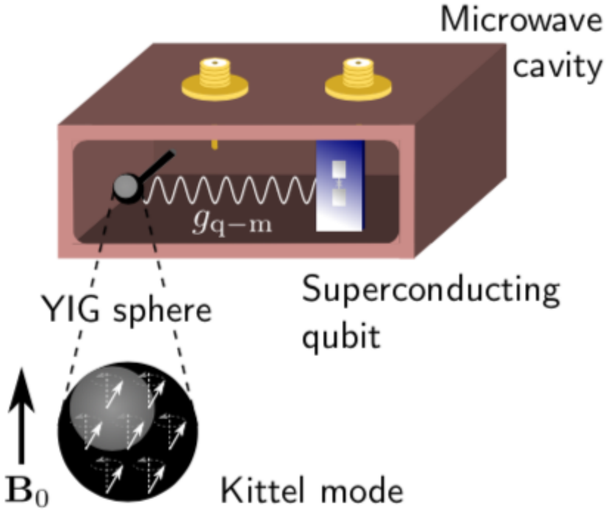

D. Lanchace-Quirion *et al.*, APE **12**, 7 (2019)

Master's project

- Characterization of ferromagnetic resonance (FMR) in different samples in quantum regime using microwave spectroscopy
  - → Comparison of FMR at room and mK temperatures
  - → Possible coupling of ferromagnetic thin films with superconducting resonators at mK

Room temperature setup

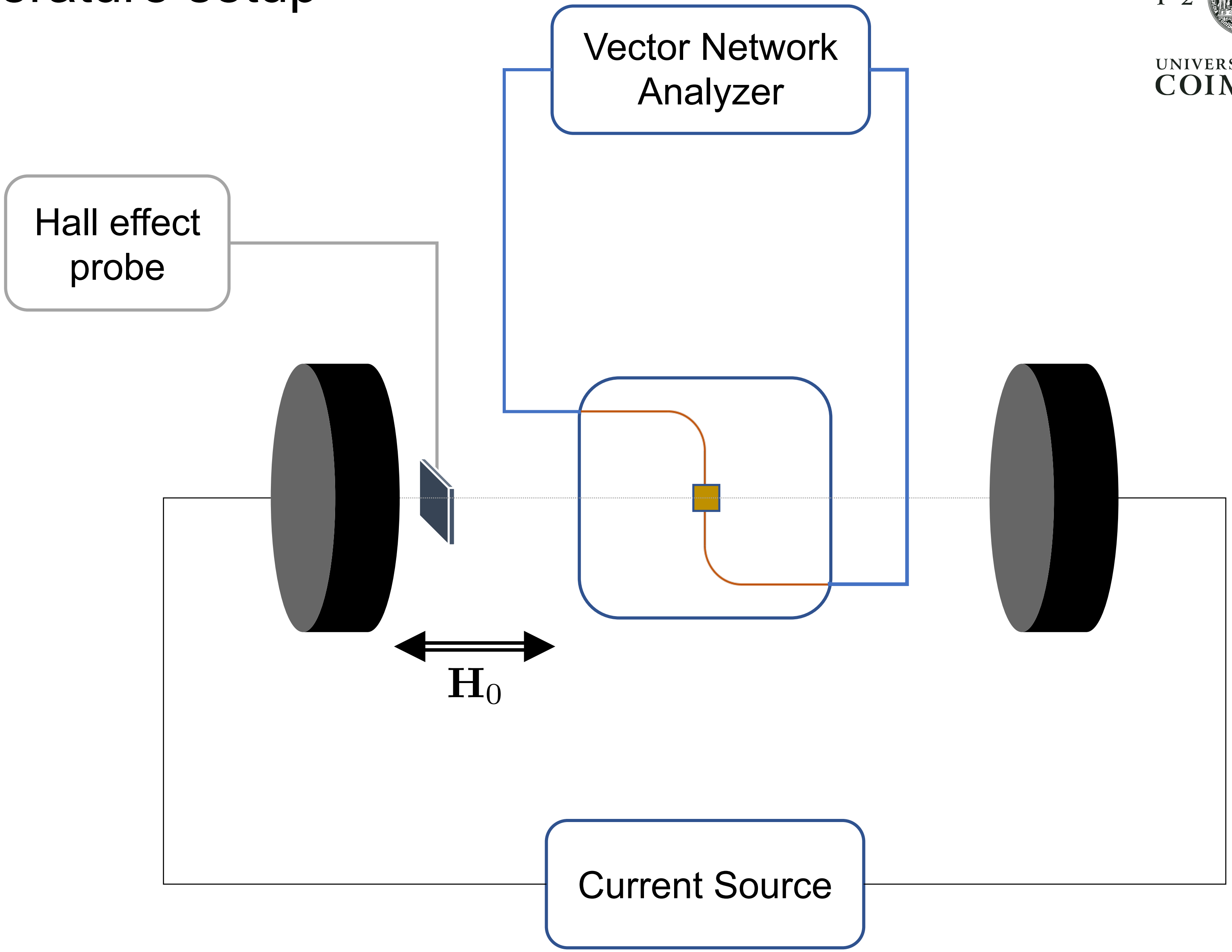

Room temperature setup

Vector Network Analyzer (VNA)

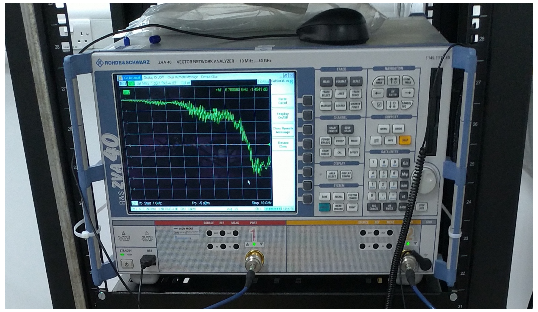

Magnet w/ sample

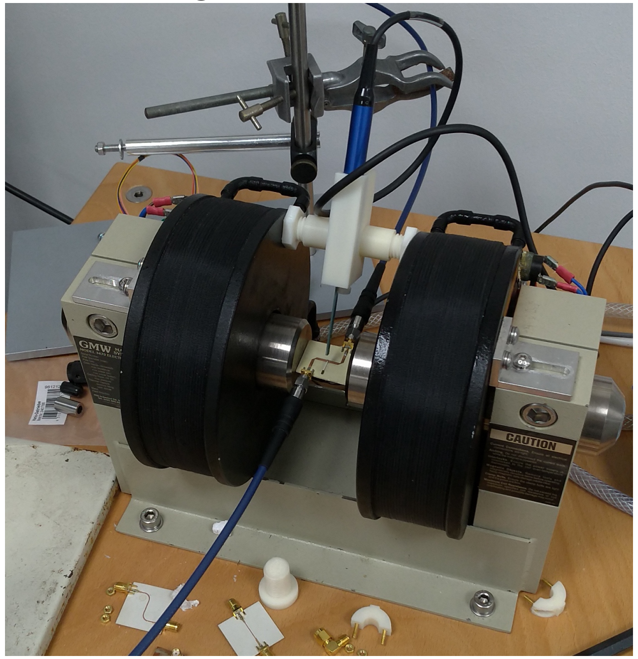

Current source

Hall effect sensor

1 2 9 0
UNIVERSIDADE D COIMBRA

University of Glasgow

Room temperature setup

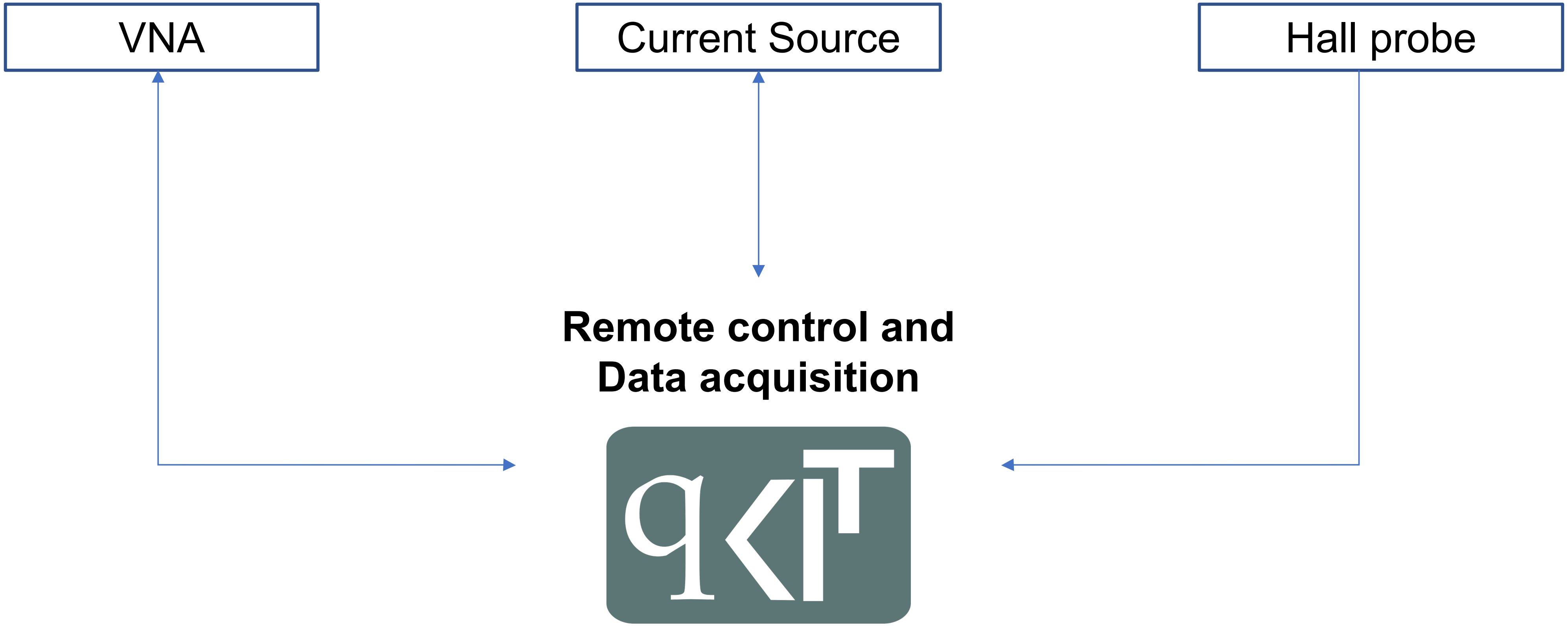

https://github.com/qkitgroup/qkit

YIG sphere 0.5 mm

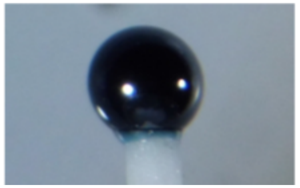

Y. Tabuchi *et al.*, PRL **113**, 083603 (2014)

1 2 9 0
UNIVERSIDADE D COIMBRA

University of Glasgow

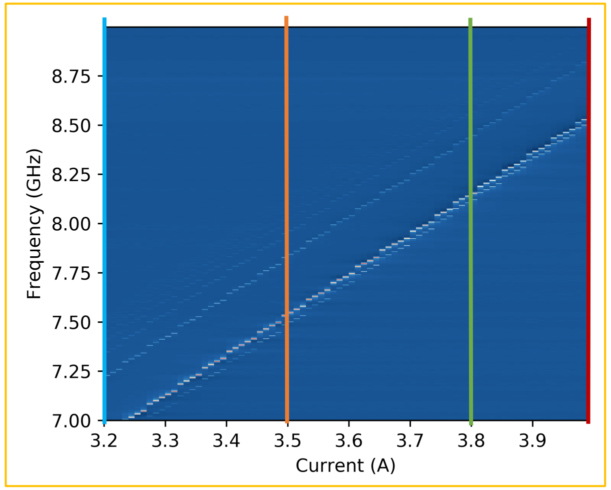

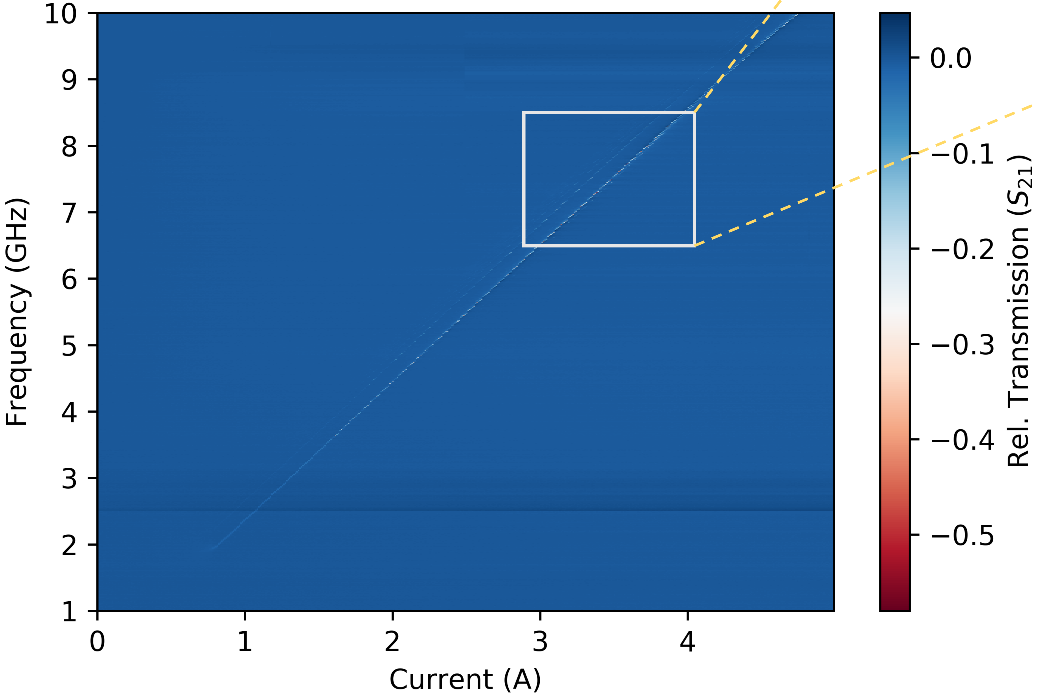

$$\omega = \gamma H_0$$

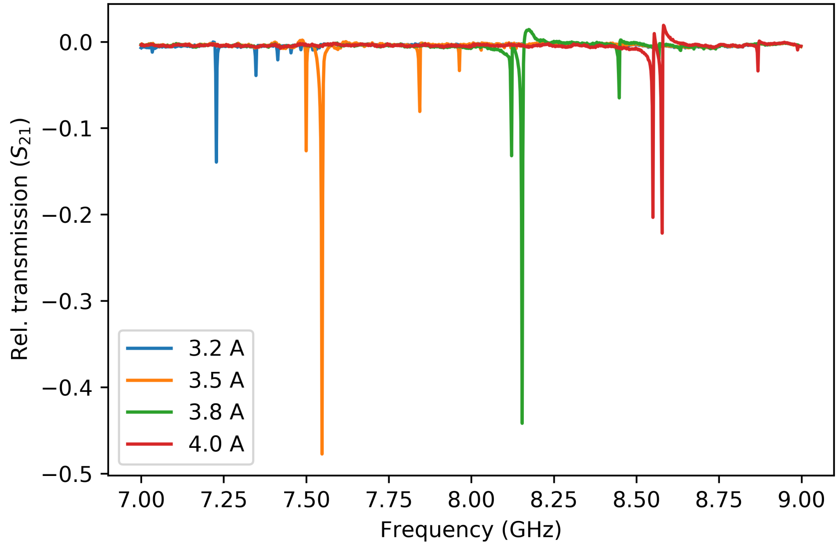

Permalloy thin film (80 nm)

University of Glasgow

1 2 9 0 UNIVERSIDADE D COIMBRA

0 dBm

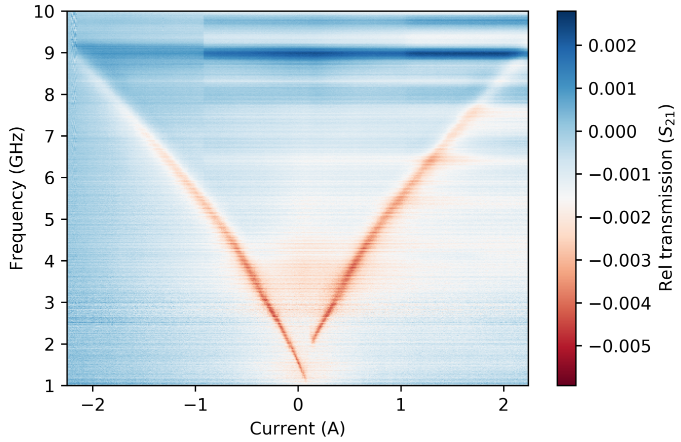

5 dBm

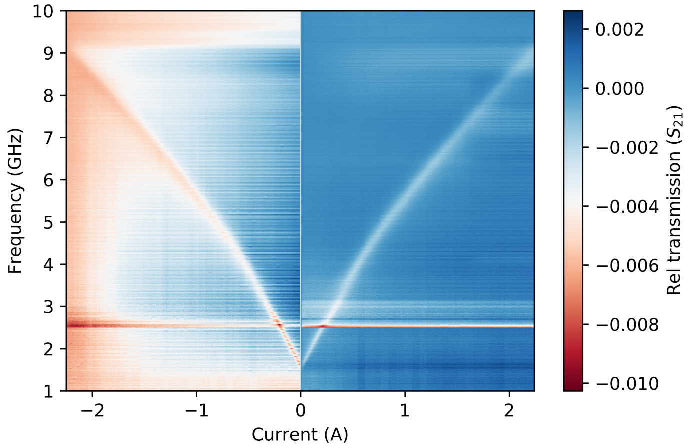

-5 dBm

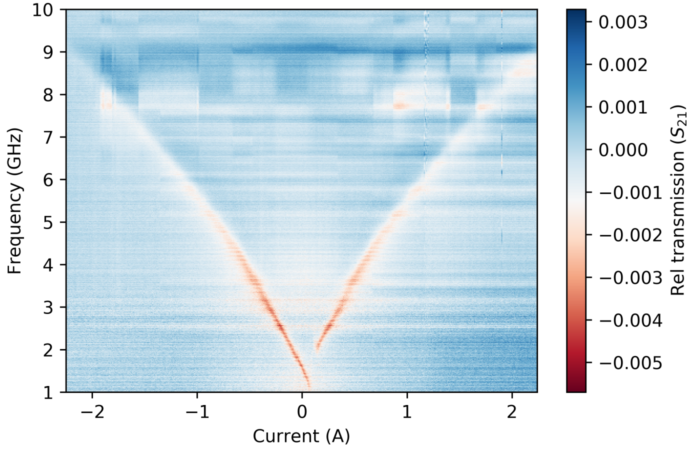

-20 dBm

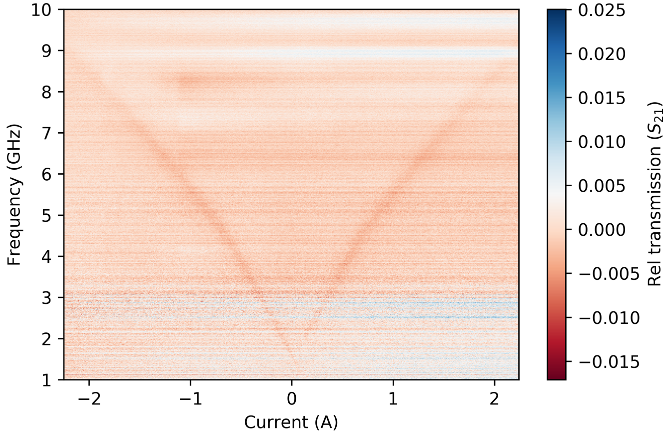

Permalloy thin film (80 nm)

Negative to positive current sweep (-5 dBm)

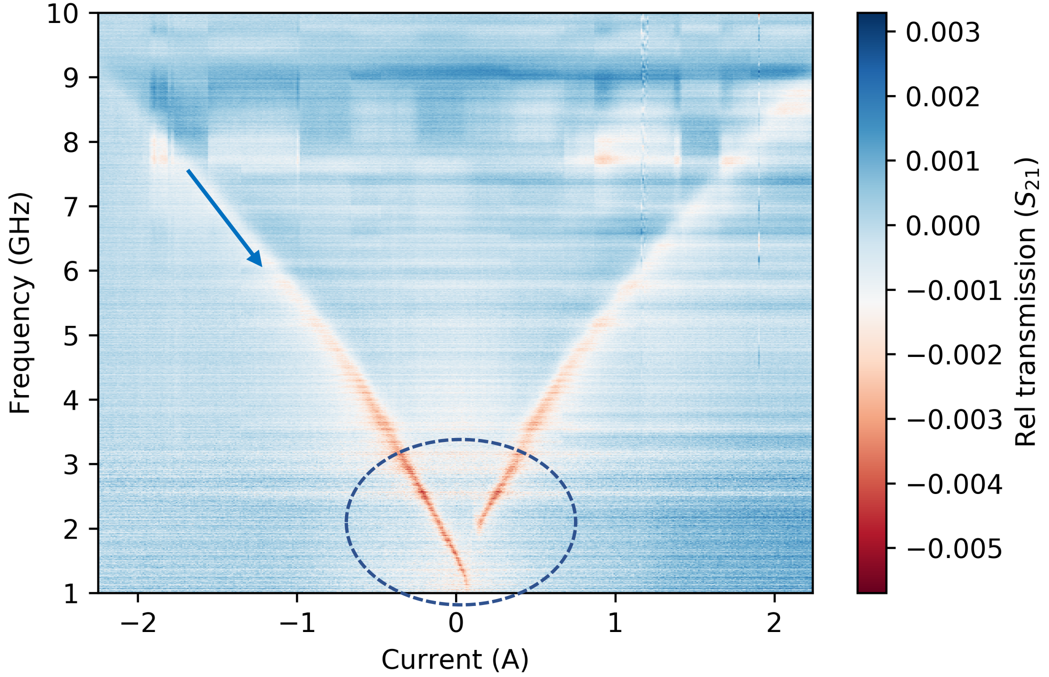

Positive to negative current sweep (+ 5dBm)

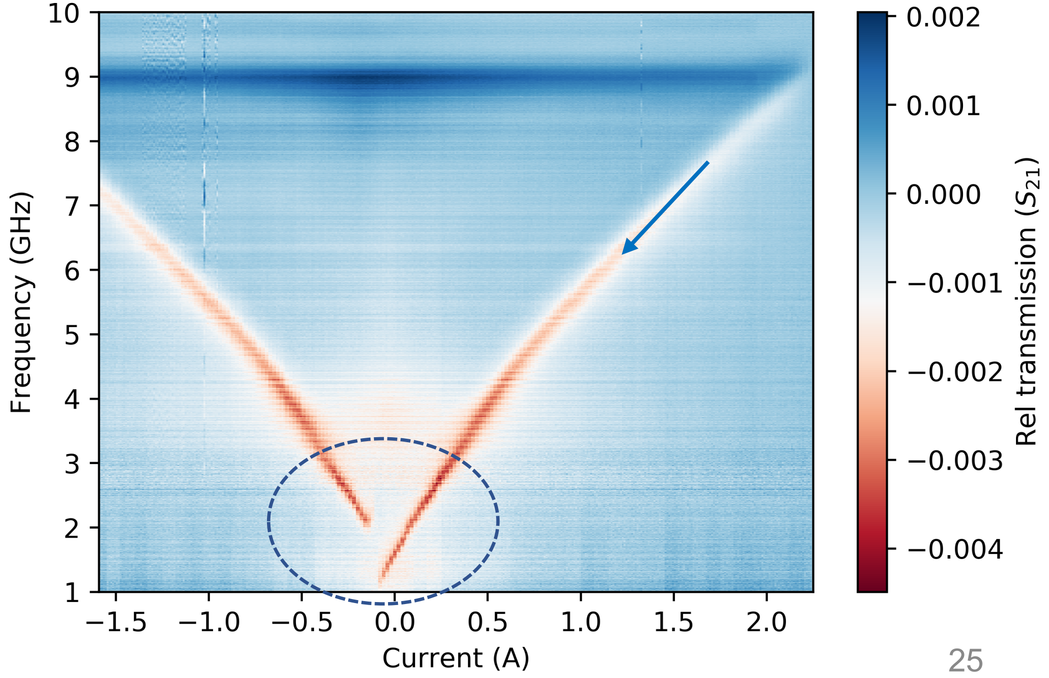

YIG thin film (0.99 μm)

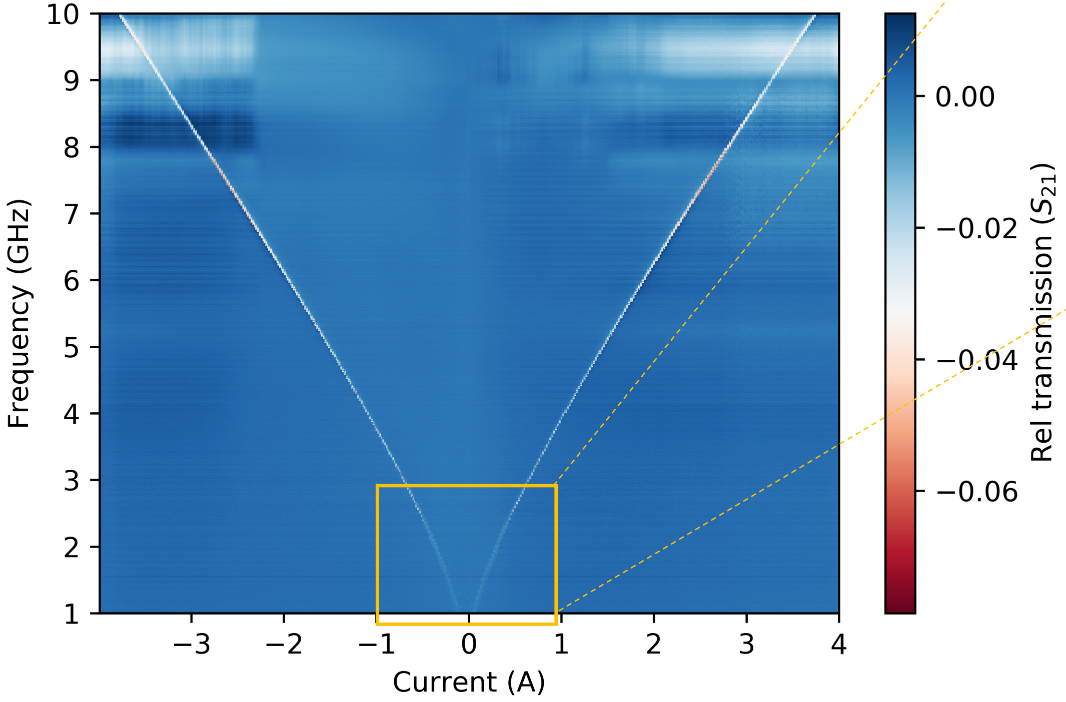

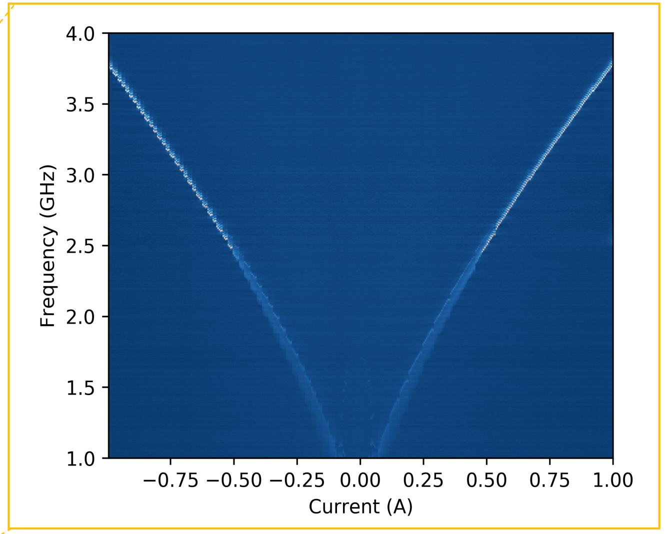

90º rotation

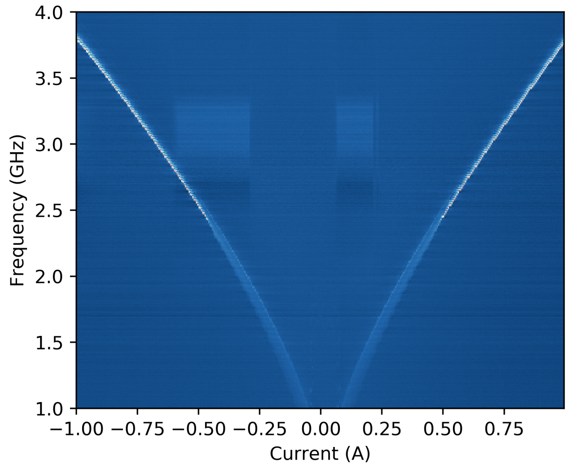

$$\omega = \gamma \sqrt{H_0 \left(H_0 + \mu_0 M\right)}$$

1 2 9 0
UNIVERSIDADE D
COIMBRA
University of Glasgow

YIG thin film (0.99 μm)

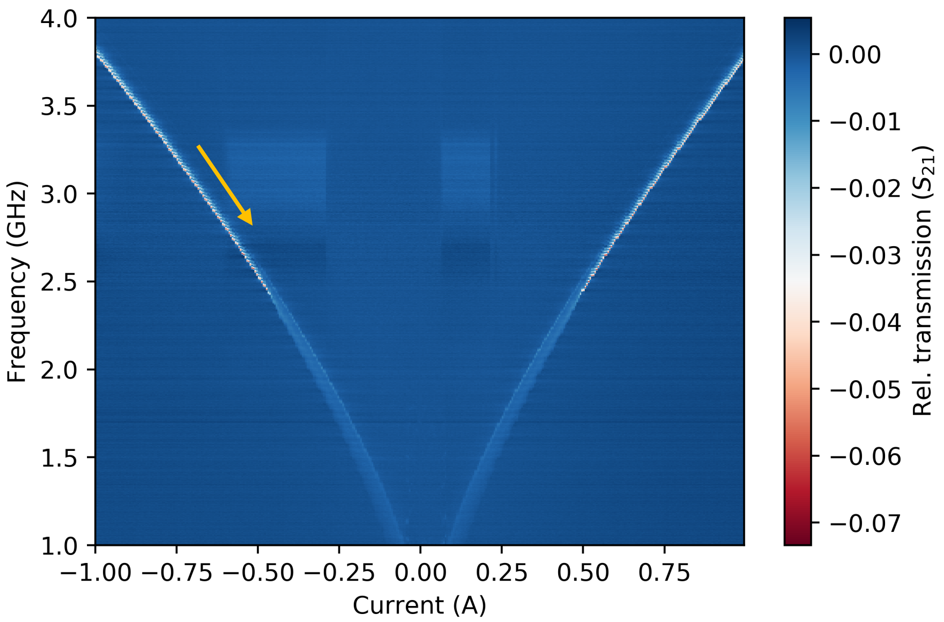

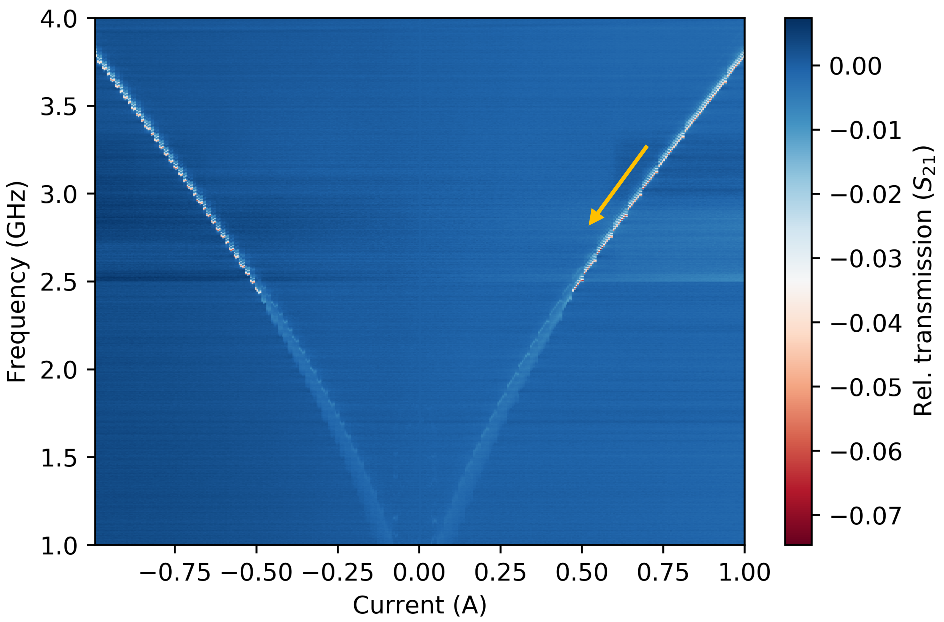

mK setup

1 2 9 0
UNIVERSIDADE D COIMBRA
University of Glasgow

Adiabatic Demagnetization Refrigerator (ADR)

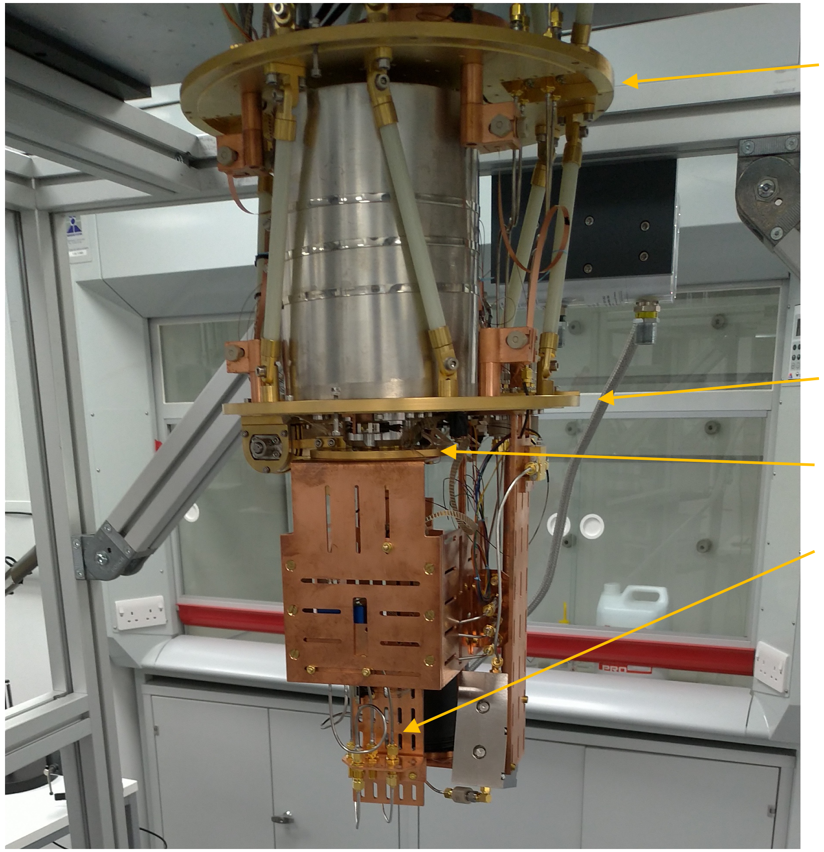

70 K

4 K

0.5 K

0.03 K

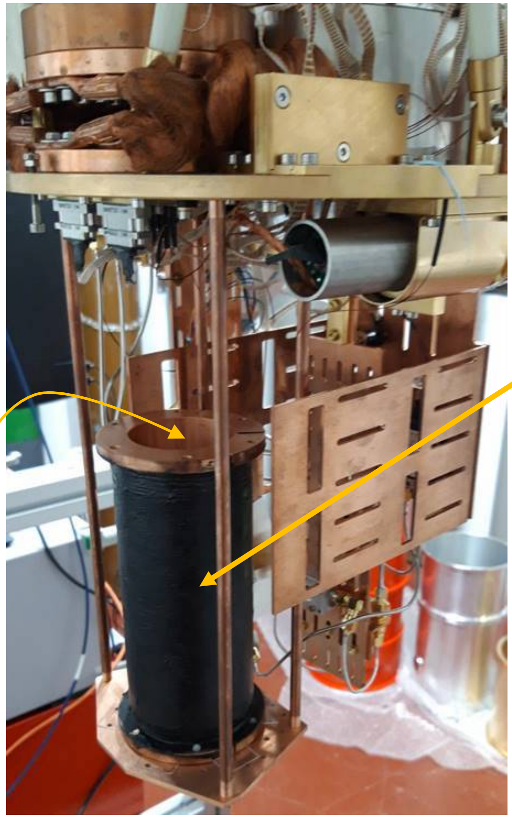

Sample

Solenoid

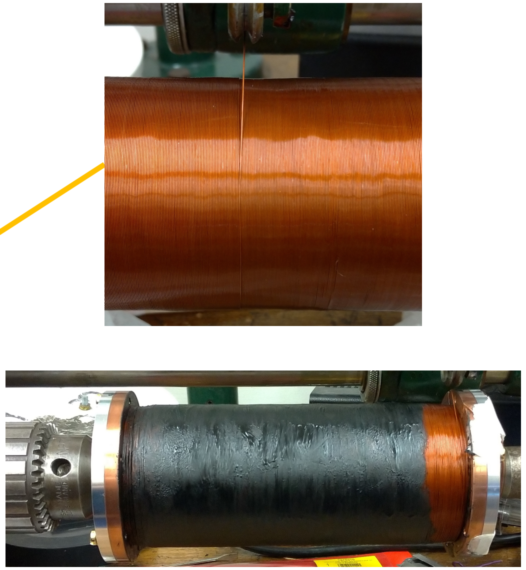

mK setup

Solenoid calibration

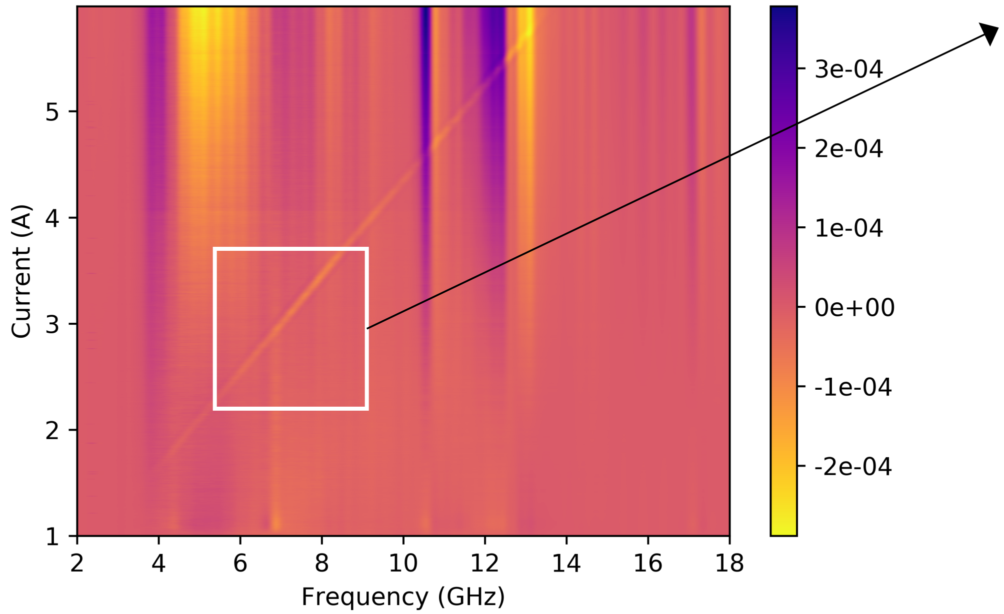

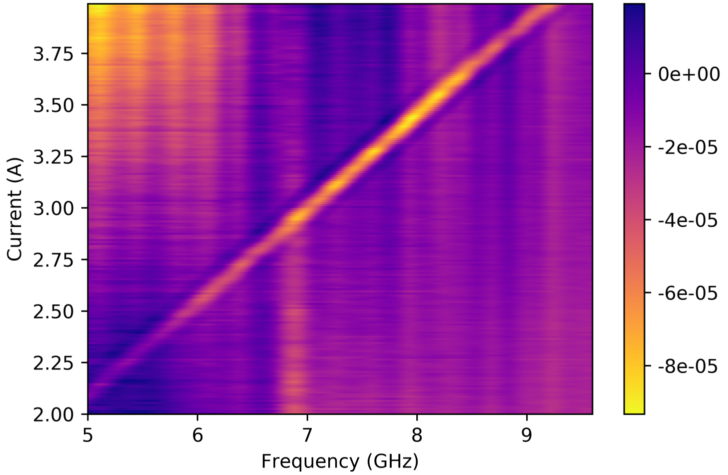

- DPPH sample + SC resonator
- Paramagnetic resonance at ~4K
- Current to field ratio: ~79 mT/A
  - Expected value: 83 mT/A

What's next

- Further analysis of room temperature data
- FMR measurements at mK temperatures
  - YIG thin film and sphere
  - Comparison between measurements
- YIG+resonator measurements at mK